Research Article / Review Article FUPRE JOURNAL 8(4): 69-89(2024)

FUPRE Journal

of

Scientific and Industrial Research

ISSN: 2579-1184(Print) ISSN: 2578-1129 (Online)

http://fupre.edu.ng/journal

Impact of Velocity Index and Significance of Nanofluid Flow of Magnetohydrodynamics (MHD) over a Stretching-Porous Sheet with Dufour and Ohmic Heating Effects

DAMISA, J.[1,*], *OKEDOYE, A. M.* [2]

[1]*Department of Mathematics, Federal University of Petroleum Resources, Effurun, Nigeria*

ARTICLE INFO

Received: 09/05/2024
Accepted: 10/10/2024

Keywords

Dufour, Index velocity, MHD, Nanofluid, Ohmic heating, Porous Sheet, Stretching sheet

ABSTRACT

This paper "impact of velocity index and significance of nanofluid flow of magnetohydrodynamics (MHD) over a stretching-porous sheet with dufour and Ohmic Heating Effects" is aimed at analysing the effect of velocity index with dufour and ohmic heating parameter on the flow of nanofluid. Also, it examines the significant effect of nanofluid thermophysical properties on fluid flow. Velocity index of fluid flow is referred to as the ratio of the actual velocity of the fluid at a specific point to the average velocity. With this in view, the effect of velocity index is examined on the fluid flow. The nanofluid under consideration is the copper (Cu) with base fluid as water (H_2O). The partial differential equations governing the nanofluid flow are transformed with the use stream functions and similarity variables. The transform equation is solved numerically using MAPPLE for various values of the controlling parameters of the flow. The results are presented in graphs and tables. Based on the observations, it is worth noting that the presence of the velocity index parameter *(m)* leads to the increase in the velocity of the fluid flow and the nanofluid thermophysical properties inculcated into the flow shows a significant effect on the flow of fluid. It is also worth noting that the increase in the buoyancy due to temperature *(Gt)* causes the temperature to increases at the wall and decreases along the free stream.

1. INTRODUCTION

In the field of fluid mechanics, it is a well-known fact that gaseous and liquid state of matter are regarded as fluid. The velocity of these fluids are of great importance in science and engineering. The velocity index is considered to have a vast significance in the drilling at various aspects. This provides insight into the distribution of fluid velocity helping the engineers to optimize flow conditions for various industrial ad engineering purposes. Johnson and Cowen (2017) examined the remote determination of the velocity index and mean streamwise velocity profiles, in this study, it is revealed that the open channel flow is well approximated by power law and that the remote predictions of surface and friction velocity leads to predictions of depth-averaged velocity. Koriko *et al.* (2017) studied the analysis of boundary layer formed on an upper horizontal surface of a paraboloid of revolution within nanofluid flowin the presence of thermophoresis and Brownian motion of 29nm Cuo. In the study they considered a nanofluid flow past an upper horizontal surface of a paraboloid of revolution in the presence of space dependent internal heat source and thermal radiation. Also, they consider the velocity power index relating to the stretching sheet. It is revealed in the study that the increase

*Corresponding author, e-mail:damisajohn226@gmail.com
DIO
©Scientific Information, Documentation and Publishing Office at FUPRE Journal

in the velocity power index brings about the increase in the vertical velocity and the temperature of the fluid, while a decrease in the horizontal velocity.

Buoyancy force is the upward force exerted on an object which is completely or partially immersed in a fluid. This upward force can also be regarded as upthrust. Buoyancy has wide application in fluid mechanics, it plays vital roles in the motion of fluid and as such several researchers has carried out significant effects on the vital role in several industries and motion of fluid in various categories. Kalaivanan *etal* (2021), discussed buoyancy driven flow of a secod-grade nanofluid flow taking into consideration the Arrhenius activation energy and elastic deformation model and numerical results. In the study, it is shown that an increase in the buoyancy due to temperature and concentration leads to the increase in Nusselt number and a decrease in the local Sherwood number. Buoyancy force plays a vital role in the flow of fluid as earlier stated. This has a significant impact in several industrial processes. It is observed that when the weight of an object is equal to the buoyancy force, it tends to float. Hassan (2017), examined an overview of computational fluid dynamics and nuclear application.

Magnetohydrodynamics (MHD) is the study of fluid motion with the aids of electrical current in conjunction with magnetic field. This describes the general means of electrically conducting fluid flow in collaboration with magnetic field. Researchers over the years has shown great interest in the study of MHD. Okedoye *etal*.(2022), examined the two dimensional dissipative Non-slip MHD flow of Arrhenius chemical reaction with variable properties. In the study, heat and mass transfer effect with suction or injection was considered and it is discovered that at low Reynold number, nonlinear heat and mass transfer flow ocsur close to x-axis boundary.

Nanofluids over the years has been greatly proven by researchers the effectiveness in terms of heat transfer application due to thermophysical properties. The significance of nanofluid cannot be over emphasized as they are known for their capability of thermal conductivity as useful for industrial uses. Bhavin *etal*. (2022) examined the synthesis, stability, thermophysical properties and heat transfer and came out with the conclusion that nanofluid possesses excellent thermophysical properties such as thermal conductivity, dynamic viscosity, density and specific heat capacity which attracts its usefulness in various heat transfer application such as solar thermal systems, refrigeration system, boiling application and then stated and then stated some drawback as related to its long-term stability. Nanofluids are said to also possess electrical, optical and tri-biological properties. Volizade *etal* (2019) and with ten times increase in the concentration of the nanofluid, the extinction coefficient of the nanofluid was increase to 17% optical properties of gold and silver. Basically, nanofluid enhances performanceof fluid flow and heat transfer in several industrial processes. This is contained in Xian and Qiang (2000) who analysed the heat transfer enhancement of nanofluid and concluded that the volume fraction dimension and properties of the nanoparticles affects the thermal conductivity of the nanofluid.

Stretching surface is associated with corresponding increase of the component of fluid flow along a path or direction of the fluid flow. The stretching surface comes with several industrial usefulness cutting across the condensation procedures of metallic plate, polymer sheet extrusion from a dye, aerodynamic extrusion of a plastic sheet. Javad and Sina (2012) analysed the viscous flow over nonlinear stretching sheet with effect of viscous dissipation, in this study, It is discovered that with the increase in the prandtl number,

there is a decrease in the thermal boundary layer thickness and that the thickness of thermal boundary layer is greater than that of the velocity boundary layer and at the end of the thermal boundary layer in which velocity gradient is reduced to zero. Also, Vikas Poply (2022) examined the heat transfer in an MHD nanofluid over a stretching sheet. From the findings, the skin friction coefficient increases with the increase in the magnetic parameter (M) which is also in line with the current study. On the hand, by the term porous media, it means material or surfaces wit void or surfaces with pore structure which are typically fluid filled in biological application. Porous media in fluid flow comes with several and useful application such as oil and gas reservoir simulation, enhance oil recovery carbon dioxide sequestration and water soil infilteration. Shankar and Eshetu (2014) studied the Heat and Mass Transfer through a Porous Media of MHD Flow of Nanofluid with Thermal Radiation, Viscous Dissipation and Chemical Reaction Effect.

Considering the several literatures above, it is discovered that Shankar and Eshetu (2014) examined Heat and Mass Transfer through a Porous Media of MHD Flow of Nanofluids with Thermal Radiation, Viscous Dissipation and Chemical Reaction Effects and Koriko *et al* (2017) who analysed analysis of boundary layer formed on an upper horizontal surface of a paraboloid of revolution within nanofluid flow in the presence of thermophoresis and brownian motion of 29 nm Cuo and mhd boundary layer flow of nanofluid through a porous medium over a stretching sheet with variable wall thickness. This study will focus on the impact of velocity index and significance of nanofluid flow of magnetohydrodynamics (MHD) over a stretching-porous sheet with dufour and Ohmic heating effects.

2. Mathematical Model

Consider a flow of two-dimensional steady laminar boundary layer flow of Cu-water nanofluid over a stretching porous sheet. The *x-axis* is taken along the direction of the continuous stretching surface and the *y-axis* is measured normal to the surface of the sheet. A uniform transverse magnetic field of strength B_0 is applied in the direction of *y-axis*. The flow is continuous due to stretching of the sheet; Following the assumptions of Koriko *et al* (2017), the domain of flow between $A(x+b)^{\frac{1-m}{2}} \leq y < \infty$ for which y could be varied by plotting the graph of $y = A(x+b)^{\frac{1-m}{2}}$ against x using $b = 1$ and $m = 0.25$ with a stretching parallel velocity $U_w = U_0(x+b)^m$. It is also assumed that the flow does not start from the origin, hence, the starting point of the flow is a function $y = A(x+b)^{\frac{1-m}{2}}$, the temperature of the horizontal surface with variable thickness is of the form $T_w = A(x+b)^{\frac{1-m}{2}}$ when m is the velocity power index, b is the parameter relating to the stretching sheet, $T_\infty$is the fluid has ambient temperature, also, the concentration of the horizontal surface with variable thickness is of the form $C_w = B(x+b)^{\frac{1-m}{2}}$, C_∞ is the fluid has ambient concentration. The Dufour and ohmic heating effects with a modified natural buoyancy model force similar to that in Makinde and Animasaun (2016) is incorporated into the flow formulation.

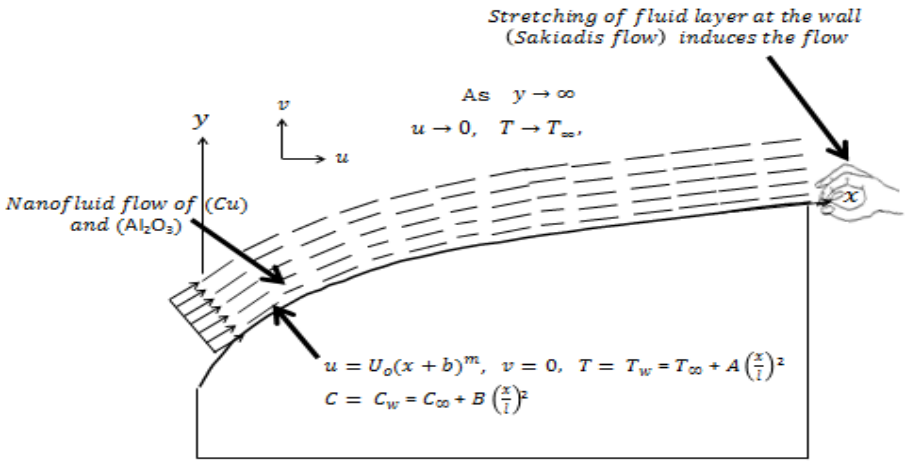

Figure 1: Flow configuration and coordinate system (Koriko *et al* (2017)**)**

$$\frac{\partial u}{\partial x} + \frac{\partial v}{\partial y} = 0 \tag{1}$$

$$u\frac{\partial u}{\partial x} + v\frac{\partial u}{\partial y} = \frac{\mu_{nf}}{\rho_{nf}}\frac{\partial^2 u}{\partial y^2} - \frac{\sigma\beta_0^2}{\rho_{nf}}u - \frac{\mu_{nf}}{\rho_{nf}}\frac{1}{k}u + \frac{g\beta_t}{\rho_{nf}}\frac{m+1}{2}(T - T_\infty) + \frac{g\beta_C}{\rho_{nf}}\frac{m+1}{2}(C - C_\infty) \tag{2}$$

$$u\frac{\partial T}{\partial x} + v\frac{\partial T}{\partial y} = \alpha_{nf}\frac{\partial^2 T}{\partial y^2} - \frac{1}{(\rho c_p)_{nf}}\frac{\partial q_r}{\partial y} + \frac{\mu_{nf}}{(\rho c_p)_{nf}}\left(\frac{\partial u}{\partial y}\right)^2 + \frac{D_m k_{nf}}{C_s C_p}\frac{\partial^2 C}{\partial y^2} + \frac{\sigma\beta_0^2}{(\rho c_p)_{nf}}u^2 \tag{3}$$

$$\rho_{nf}\left(u\frac{\partial C}{\partial x} + v\frac{\partial C}{\partial y}\right) = \frac{D_m k_t}{C_s C_p}\frac{\partial^2 C}{\partial y^2} + \frac{D_m k_{nf}}{\tau}\frac{\partial^2 T}{\partial y^2} - k_0(C - C_\infty) \tag{4}$$

where u and v are the velocity component in the x and y direction respectively. β_T is the volumetric coefficient of thermal expansion of nanofluid, T is the temperature, C is the concentration of the nanofluid, C_∞ is the ambient concentration, q_r is the radiative heat flux, D_m is the mass diffusivity, k_t is the thermal diffusion ratio C_s is the concentration susceptivity, C_p is specific heat at constant pressure, τ is the thermophoretics, B_0 is the magnetic field, k is the permeability of the porous medium, k_0 is the chemical reaction and σ is the electrical conductivity. The dynamic viscosity of the nanofluid (μ_{nf}), effective density of the nanofluid (ρ_{nf}), thermal conductivity of the nanofluid (α_{nf}) and heat capacitance of the nanofluid $(\rho c_p)_{nf}$ (Shankar and Eshetu, 2014);

$$\left.\begin{aligned} \rho_{nf} &= (1-\phi)\rho_f + \phi\rho_s \\ \alpha_{nf} &= \frac{k_{nf}}{(\rho c_p)_{nf}} \\ \mu_{nf} &= \frac{\mu_f}{(1-\emptyset)^{2.5}} \\ (\rho c_p)_{nf} &= (\rho c_p)_f \left((1-\phi) + \phi \frac{(\rho c_p)_s}{(\rho c_p)_f} \right) \end{aligned}\right\} \quad (5)$$

The thermal conductivity of nanofluid of a spherical Nanoparticle (Shankar and Eshetu, 2014) is given as:

$$k_{nf} = k_f \left[\frac{k_s + 2k_f - 2\emptyset(k_f - k_s)}{k_s + k_f - \emptyset(k_f - k_s)} \right] \quad (6)$$

Where f and s are the subscript of the quantities in the base fluid and nanoparticles respectively. According to the Roseland diffusion approximation Husseini (2013) and Raptis (1998) the radiative heat flux q_r is given by

$$q_r = -\frac{4\sigma^*}{3k^*}\frac{\partial T^4}{\partial y} \quad (7)$$

Where σ^* and k^* are the Stefan-Boltzmann constant and the Rosseland mean absorption coefficient respectively. We assumed that the temperature difference within the flow are sufficiently small such that T^4 may be expressed as a linear function of temperature.

$$T^4 \approx 4T_\infty^3 T - 3T_\infty^4 \quad (8)$$

Substituting Equation (8) into Equation (7) and differentiate with respect to y, we have;

$$q_r = -\frac{4\sigma^*}{3k^*}\frac{\partial}{\partial y}(4T_\infty^3 T - 3T_\infty^4) = -\frac{4\sigma^*}{3k^*}4T_\infty^3\frac{\partial T}{\partial y} = -\frac{16\sigma^* T_\infty^3}{3k^*}\frac{\partial T}{\partial y}$$

$$\frac{\partial q_r}{\partial y} = -\frac{16\sigma^* T_\infty^3}{3k^*}\frac{\partial^2 T}{\partial y^2} \quad (9)$$

Substituting (9) into (3), we have

$$u\frac{\partial T}{\partial x} + v\frac{\partial T}{\partial y} = \frac{\alpha_{nf}}{(\rho c_p)_{nf}}\frac{\partial^2 T}{\partial y^2} - \frac{16\sigma^* T_\infty^3}{3k^*(\rho c_p)_{nf}}\frac{\partial^2 T}{\partial y^2} + \frac{\mu_{nf}}{(\rho c_p)_{nf}}\left(\frac{\partial u}{\partial y}\right)^2 + \frac{D_m k_{n_f}}{C_s C_p}\frac{\partial^2 C}{\partial y^2} + \frac{\sigma\beta_0^2}{(\rho c_p)_{nf}}u^2 \quad (10)$$

The appropriate boundary conditions for the problem are:

$$u = U_W = U_0(x+b)^m, v = 0, T = T_w(x), C = C_w(x) \ at\ y = A(x+b)^{\frac{1-m}{2}}$$
$$u \to 0, T \to T_\infty, C \to C_\infty \ as\ y \to \infty \quad (11)$$

Provided that *A, B and b* are constant, $b > 0$ A and B are the area of emitting body of the temperature and concentration equation respectively and l is the characteristics length.

2.1 Method of Solution

We seek a similarity solution using the stream functions similar to Koriko *et al* (2017) with the longitudinal and axial component of the velocity, u and v define as;

$$\left.\begin{aligned}
\psi &= f(\eta)\sqrt{\left(\frac{2(\vartheta_{nf}U_0)}{m+1}\right)}(x+b)^{\frac{m+1}{2}} \\
\eta &= y\sqrt{\left(\frac{m+1}{2}\frac{U_0}{\vartheta_{nf}}\right)}(x+b)^{\frac{m-1}{2}} \\
T_w(x) &= A(x+b)^{\frac{1-m}{2}} \\
C_w(x) &= B(x+b)^{\frac{1-m}{2}} \\
u &= U_0(x+b)^{\frac{m+1}{2}}f'(\eta) \\
v &= -\frac{m+1}{2}\left(\sqrt{\left(\frac{2(\vartheta_{nf}U_0)}{m+1}\right)}(x+b)^{\frac{m+1}{2}}\right)f(\eta)
\end{aligned}\right\} \quad (12)$$

And the similarity variables for energy and species concentration are defined as:

$$\theta(\eta) = \frac{T-T_\infty}{T_w(x)-T_\infty}, \Theta(\eta) = \frac{C-C_\infty}{C_w(x)-C_\infty} \quad (13)$$

Using equations (12) and (13) in equations (1), (2), (4) and (10), we the non-dimensional momentum, energy and chemical species concentration as;

$$f'''(\eta) + \phi_1\left(f(\eta)f''(\eta) - \left(f'(\eta)\right)^2 - M\left(\frac{2}{m+1}\right)f'(\eta) + f(\eta)f''(\eta) - \left(f'(\eta)\right)^2 - M\left(\frac{2}{m+1}\right)f'(\eta)\right) - \left(\frac{2}{m+1}\right)k_1 f'(\eta) = 0 \quad (14)$$

$$\left(1+\frac{4R}{3}\right)\theta''(\eta) + Pr\phi_3\frac{k_f}{k_{nf}}\left\{f(\eta)\theta'(\eta) - \left(\frac{1-m}{m+1}\right)f'(\eta)\theta(\eta) + \frac{Ec}{\phi_3}\left(f''(\eta)\right)^2 + \left(\frac{1}{m+1}\right)\frac{M(Ec)}{\phi_4}\left(f'(\eta)\right)^2 + Du\Theta''(\eta)\right\} = 0 \quad (15)$$

$$\Theta''(\eta) + \phi_2 Sc\left(f(\eta)\Theta'(\eta) - \left(\frac{1-m}{m+1}\right)f'(\eta)\Theta(\eta)\right) - Sc\gamma\left(\frac{2}{m+1}\right)\Theta(\eta) + Sr\theta''(\eta) = 0 \quad (16)$$

It is important to take into consideration when non-dimensionalising the boundary conditions that$y \neq 0$ (i.e. the minimum value is not at the origin). Which connotes that setting $y = 0$ is not proper or valid, but using the start point at $y = A(x+b)^{\frac{1-m}{2}}$ as the minimum value which corresponds to $\eta = y\sqrt{\left(\frac{m+1}{2}\frac{U_0}{\vartheta_{nf}}\right)}(x+b)^{\frac{m-1}{2}}$. At the wall, the boundary condition appropriate to scale the boundary layer flow can be expressed as;

$$\eta = A(x+b)^{\frac{1-m}{2}}\sqrt{\left(\frac{m+1}{2}\frac{U_0}{\vartheta_{nf}}\right)}(x+b)^{\frac{m-1}{2}}$$

Let;

$$\lambda = A\sqrt{\left(\frac{m+1}{2}\frac{U_0}{\vartheta_{nf}}\right)}$$

Hence, at the domain of $[\lambda, \infty]$ the associated boundary conditions becomes;

$$\begin{aligned} f(\lambda) = \lambda\left(\frac{1-m}{m+1}\right), f'(\lambda) = 1, \theta(\lambda) = 1, \Theta(\lambda) = 1 \quad at\ \eta\ = \lambda \\ f'(\infty) \to 0, \theta(\infty)\ \to 0, \Theta(\infty) \to 0 \qquad\qquad as\ \eta \to \infty \end{aligned} \tag{17}$$

Where

$$\left.\begin{aligned} Pr = \frac{(\mu c_p)_f}{k_f}, Du = \frac{D_m k_f}{C_s C_p}\frac{(C_w - C_\infty)}{(T_w - T_\infty)}\frac{1}{\nu_f}, Ec = \frac{1}{k_t}\frac{U_0}{(T_w - T_\infty)x^2 c_{p_f}}, k_1 = \frac{\nu_f}{bk}, \\ Gr_t = \frac{g\beta_T}{U_0\rho_f}(T_w\ - T_\infty),\ Gr_c = \frac{g\beta_c}{U_0\rho_n}\ (C_w - C_\infty)\ , Re_x = \frac{xu_w}{\upsilon_f}, R = \frac{4\sigma^* T_\infty^3}{k^* k_f k_t}, \\ Sc = \frac{\nu_{nf}}{D_m}, \gamma = \frac{C_s C_p}{k_t}\frac{k_0}{U_0}, Sr = \frac{D_m k_t}{C_s C_p}\frac{(T_w - T_\infty)}{(C_w - C_\infty)}, A = (T_w - T_\infty)l, B = (C_w - C_\infty)l \end{aligned}\right\} \tag{18}$$

The dimensionless non-linear system of equation (14), (15) and (16) with the boundary conditions (17) are the functions of η depending λ. For the purpose of easy computation, it would be required that the domain $[\lambda, \infty]$ be transformed to the domain $[0, \infty]$ as $F(\chi) = F(\eta - \lambda) = f(\eta), G(\chi) = G(\eta - \lambda) = \theta(\eta), \mathrm{H}(\chi) = \mathrm{H}(\eta - \lambda) = \Theta(\eta)$. Hence, the dimensionless non-linear system of the governing equation becomes;

$$\begin{aligned} F'''(\chi) + \phi_1\left(F(\chi)F''(\chi) - \left(F'(\chi)\right)^2 - M\left(\frac{2}{m+1}\right)F'(\chi) + \frac{1}{\phi_2}\left(Gr_t G(\chi) + Gr_c \mathrm{H}(\chi)\right)\right) \\ - \left(\frac{2}{m+1}\right)k_1 F'(\chi) = 0 \end{aligned} \tag{19}$$

$$\begin{aligned} \left(1 + \frac{4R}{3}\right)G''(\chi) \\ + Pr\phi_3\frac{k_f}{k_{nf}}\left\{F(\chi)G'(\chi) - \left(\frac{1-m}{m+1}\right)F'(\chi)G(\chi) + \frac{Ec}{\phi_3}\left(F''(\chi)\right)^2\right. \\ \left. + \left(\frac{1}{m+1}\right)\frac{M(Ec)}{\phi_4}\left(F'(\chi)\right)^2 + DuH''(\chi)\right\} = 0 \end{aligned} \tag{20}$$

$$\mathrm{H}''(\chi) + \phi_2 Sc\left(F(\chi)\mathrm{H}'(\chi) - \left(\frac{1-m}{m+1}\right)F'(\chi)\mathrm{H}(\chi)\right) - Sc\gamma\left(\frac{2}{m+1}\right)\mathrm{H}(\chi) + SrG''(\chi) = 0 \tag{21}$$

Subjected to the boundary conditions in the domain of $[0, \infty]$;

$$\begin{aligned} F(\chi) = \lambda\left(\frac{1-m}{m+1}\right), F'(\chi) = 1, G(\chi) = 1, \mathrm{H}(\chi) = 1 \quad at\ \chi\ = 0 \\ F'(\chi) \to 0, G(\chi)\ \to 0, \mathrm{H}(\chi) \to 0 \qquad\qquad as\ \chi \to \infty \end{aligned} \tag{22}$$

Rate of Flow at the wall: Engineering parameters of curiosity in the flow are skin friction coefficient C_f and Nusselt number Nu_x and local Sherwood number Sh_x defined respectively as;

$$C_f = \frac{2\tau_w}{\rho_f\sqrt{\frac{m+1}{2}}u_w^2}, \tau_w = -\mu_{nf}\left(\frac{\partial u}{\partial y}\right)_{y=A(x+b)^{\frac{1-m}{2}}}$$

Now

$$Nu_x = \frac{(x+b)q_w}{k_f(T_w(x)-T_\infty)\sqrt{\frac{m+1}{2}}}, q_w = -\left(k_{nf}+\frac{16\sigma^* T_\infty^3}{3k^*}\right)\left(\frac{\partial T}{\partial y}\right)_{y=A(x+b)^{\frac{1-m}{2}}}$$

And

$$Sh_x = \frac{(x+b)J_w}{D(C_w(x)-C_\infty)}, J_w = -D\left(\frac{\partial C}{\partial y}\right)_{y=A(x+b)^{\frac{1-m}{2}}}$$

Thus

The above equations (23) – (25) indicates that the *skin friction coefficient (surface drag)*, rate of heat transfer at the wall and rate of mass transfer at the wall respectively.

Hence,

$$C_f = -\frac{2f''(0)}{(1-\phi)^{2.5}} \quad (23)$$

$$Nu_x = -\sqrt{Re_x}\left(1+\frac{4R}{3}\right)\theta'(0) \quad (24)$$

$$Sh_x = -\sqrt{Re_x}\Theta'(0) \quad (25)$$

Table 1: Thermo-physical properties of water, copper and Alumina, Motsumi

Physical properties	Copper (Cu)	Base fluid (Water)
$C_p(JKg^{-1}k)$	385	4179
$\rho(kg/m^3)$	8933	997.1
$\kappa(W/mK)$	400	0.613
$\rho C_p(Jkg^{-1}kkg/m^3)$	3439205	4,166,880.9

3. Results and Discussion

3.1 Validity of Results

If we let $m = 1$ we recover the model in Okedoye *et al.* (2022)

Table 2: Standard values for the governing parameters

Parameter	R	Grc	Grt	M	ϕ	S_G	γ	k_1	Ec	Sc	Pr	Du	Sr
Value	2	5	10	0.5	1	3.4	0.08	1	1	0.6	0.71	0.5	0.2

Using the values in Table 1 and varying other parameters as shown in the table below, we compare our results with that of Okedoye *et al.* (2022)

Table 3: Comparison of our result with that of Okedoye et al. (2022)

	Okedoye et al. (2022)			**Current Work**		
Parameter	$f'(0)$	$\theta'(0)$	$\phi'(0)$	$f'(0)$	$\theta'(0)$	$\phi'(0)$
R=0.0	2.25859	-1.10069	-1.42527	2.2585883	-1.1006891	-1.4252673
R=0.5	2.44407	-0.88041	-1.48702	2.4440567	-0.8804110	-1.4870387
R=1.0	2.56163	-0.76175	-1.52152	2.5616389	-0.7617467	-1.5215178
R=2.0	2.70973	-0.62847	-1.56073	2.7097612	-0.6284706	-1.5607117
φ =0.0	3.35664	-0.95012	-1.37763	3.3566278	-0.9501232	-1.3776219
φ =0.2	1.67655	-0.80506	-1.57797	1.6765461	-0.8050271	-1.5779688
φ =0.4	0.46938	-0.65344	-1.71513	0.4693567	-0.6534326	-1.7151187
φ =0.8	-0.87639	-0.37634	-1.89031	-0.876323	-0.3763489	-1.8903688
Grt=0.0	-0.43338	-0.61572	-1.30999	-0.433324	-0.6157221	-1.3099092
Grt=5.0	1.67655	-0.80506	-1.57797	1.6765673	-0.8050628	-1.5779491
Grt=10.0	3.51351	-0.87565	-1.73609	3.5135516	-0.8756446	-1.7360886
Grt=15.0	7.64738	-0.90024	-2.01261	7.6473572	-0.9002452	-2.0126099

From the result of Table 3, it was observed that our result are in good agreement with that obtained by Okedoye et al.

3.2 Discussion

A closer look at the each of the figure (Fig.2 to Fig.25), shows the significant effect (enhancement) of the thermophysical properties of the nanofluid under consideration with respect to fluid flow and heat and mass transfer. Fig.2 and Fig.3 shows the effect of Soret (Sr) and stretching sheet parameter on the velocity of the fluid. It is observed that the increase in the Soret number and the stretching sheet parameter leads to the increase in the velocity of the fluid. Fig.4 and Fig.5 shows the effects of buoyancy due to concentration and the magnetic parameter respectively. From Fig.4, it is observed that the increase in the buoyancy due to concentration parameter (Gc) results in the increase of the velocity of the fluid while Fig.5, depicts the decrease in the velocity as the Magnetic parameter (M) increases. Fig.6 and Fig.7 depicts the effects of buoyancy due to temperature and velocity index (m) parameter respectively. It is observed from fig.6 that the increase in the buoyancy due to temperature leads to the increase in the velocity of the fluid. This is due to the fact that buoyancy force is an upward force exerted by fluid on an immersed object in gravity field. Hence, fluid velocity tends to increase as the buoyancy parameter is increased. On the hand, Fig.7, connotes the effect of velocity index parameter (m), from the figure, the increase in the velocity index parameter (m) also leads to the increase in the velocity of the fluid. This explain the fact that at high velocity index, there is a high tendency of more even distribution which may be desirable for several application to ensure efficiency and predictable fluid flow and at low velocity index, it suggests a more uneven flow profile which may lead to the increase in pressure drop. Fig.8 and Fig.9 shows the effect of the heat radiating parameter (R) and the Eckert number parameter (Ec) on the fluid velocity. It is observed from both figure that the increase in both parameters shows no significant effect at the wall, but yields an increasing effect on the velocity of the fluid along the free stream.

The controlling parameters also exhibit significant effect on the temperature of the fluid. Fig.10 and Fig.11 shows the effect of the Dufour number parameter (Du) and the stretching sheet parameter (λ) on the temperature of the fluid respectively. From both figures, it is observed that there is a significant increase of temperature from the

wall and all through to the free stream as there is an increase in the dufour number and the stretching sheet parameter. The dufour effect is the energy flux due to a mass concentration gradient that takes place as a result of several irreversible processes that occurs in a system. Fig. 12 depicts the effect of buoyancy due to concentration parameter (Gc), it is observed from this figure that there is a significant increase in the temperature at the wall and a decreasing effect along the free stream. Fig.13 also illustrates the effect of buoyancy due to temperature parameter (Gt). Similar observation is deduced from the previous figure. There is an increasing effect of temperature at the wall and a decreasing effect temperature at the free stream since there is an increase in the buoyancy due temperature parameter (Gt). Fig.14 and Fig.15 depict the effect of the magnetic parameter (M) and the effect of the velocity index parameter (m) on the temperature respectively. It is observed that the increase in both parameters (magnetic parameter (M) and velocity index parameter (m)), gives an increasing function of temperature at the wall and along the free stream. Fig.16 shows the effect of the radiation parameter (R) on the temperature. It is observed from the figure that there is a decreasing function of temperature at the wall and an increasing function at the free stream. fig.17 connotes the effect of the Eckert number (Ec) on the temperature. It is observed that the increase in the Eckert number parameter gives the increase in the temperature at the wall and at the free stream.

Fig.18 depicts the effect of Soret (Sr) on the concentration profile. From the figure, it is observe that at the wall, there is a decreasing function of mass transfer and an increase function of mass transfer along the free stream when there is an increase in the soret number. Fig.19 shows the effect of the stretching sheet (λ) on the concentration profile. The figure show the increasing of the concentration of the system at all point when there is an increase in the stretching sheet parameter (λ). Fig.20 and Fig.21 shows the effect of buoyancy due to concentration (Gc) and temperature (Gt) respectively. From both figures, it is observed that the increase in both parameter (Gc and Gt) leads to the decreasing function of the concentration profile. This is due to the fact that buoyancy reduces weight of an object. Fig.22 shows the effect of the magnetic parameter (M). The figure depicts the decrease in the mass transfer at the wall and an increase in the mass transfer along the free stream if there is an increase in the magnetic parameter (M). Also, Fig.23 shows the effect of the velocity index (m) on the concentration. There is an increase in the mass transfer as a result of the increase in the velocity index parameter. Fig.24 shows the effect of scaled chemical reaction parameter (γ) on Concentration disribution. From the figure, it is observed that there is a decreasing effect in the mass transfer as a result of the increase in the parameter. Fig.25 shows the effect of Eckert number (Ec) on Concentration distribution. It is observed that there is a decrease in the mass transfer at some point from the wall to a point in the free stream and a little significant increase in the mass transfer at another point in the free stream.

The table 2 below shows the value of skin friction $-F''(0)$, wall temperature gradient $-G'(0)$ and mass transfer rate $H'(0)$ for various value of Soret (Sr), Dufour (Du), stretching sheet parameter (λ), Buoyancy due to concentration (Gc), Buoyancy due to temperature (Gt), magnetic parameter (M), velocity index (m), the scaled chemical reaction parameter (γ), radiatin parameter (R), and the Eckert number (Ec). In comparison with and without the thermophysical properties of the nanofluid under consideration. From table 2 the skin friction $-F''(0)$, wall temperature gradient $-G'(0)$ and mass transfer

rate $H'(0)$ is compared with the skin friction $-F''(0)$, wall temperature gradient $-G'(0)$ and mass transfer rate $H'(0)$ of the thermophysical properties of the nanofluid gives a clear difference in value. This simply shows the fact that nanofluid enhances the perfomances of industrial processes. skin friction $F''(0)_n$, wall temperature gradient $G'(0)_n$ and mass transfer rate $H'(0)_n$ shows the influence of nanofluid thermophysical properties. From the table, it is shown that the increase in the Soret number (Sr) causes the skin friction of both $-F''(0)$ and $F''(0)_n$ with wall temperature gradient $-G'(0)$ and $-G'(0)_n$ to decrease. While the mass transfer $H'(0)$ increases. Also, the increase in the Dufour (Du) leads to the increase in the skin friction $-F''(0)$ and nanofluid skin friction $F''(0)_n$, decrease in the wall temperature of both $-G'(0)$ and $-G'(0)_n$ while the mass transfer $H'(0)$ and $H'(0)_n$ increases in function. The increase in the stretching sheet parameter (λ) also causes an increase in skin friction $-F''(0)$ and $F''(0)_n$, increase in the wall temperature $-G'(0)$ and $-G'(0)_n$ and mass transfer at the wall, decreases at some point in the free stream and increases at some point in the free stream. With the increase in the velocity index (m) leads to decrease in the skin friction ($-F''(0)$ and $F''(0)_n$) and wall temperature gradient $-G'(0)$ and $-G'(0)_n$ while an increase occur in the mass transfer $H'(0)$ and $H'(0)_n$.

Table 4 below shows the comparison of the value of skin friction $-F''(0)$ and $F''(0)_n$wall temperature gradient $-G'(0)$ and $G'(0)_n$ and mass transfer rate $H'(0)$ and $H'(0)_n$ for various value of Sr, Du, λ, Gc, Gt, M, m, γ, R, Ec

Parameter	$F(0)$	$F''(0)$	$F''(0)_n$	$G'(0)$	$G'(0)_n$	$H'(0)$	$H'(0)_n$
$Sr = 0.0$	-0.033	-0.77900	-1.23996	-0.46408	-0.91411	1.36262	1.47490
$Sr = 0.8$	-0.033	-0.80197	-1.22021	-1.88230	-0.97849	1.69684	1.84263
$Sr = 2.6$	-0.033	-0.88421	-1.19937	-13.30187	-1.05581	4.87211	2.28714
$Du = 0.0$	-0.033	-0.79425	-1.23996	-0.73983	-0.91411	1.30241	1.47490
$Du = 0.7$	-0.033	-0.76011	-1.22022	-0.83476	-0.97849	1.81052	1.84263
$Du = 1.4$	-0.033	-0.71933	-1.19937	-0.97917	-1.05582	2.58157	2.28714
$\lambda = 0.0$	-0.033	-0.96478	-1.32002	-0.84281	-0.94848	1.91408	1.71427
$\lambda = 1.0$	-0.033	-0.07542	-0.51237	-0.63977	-0.85776	0.59153	0.85740
$\lambda = 2.0$	-0.033	0.72324	0.20616	-0.77176	-0.88481	1.13993	0.78445
$Gc = 0.0$	-0.033	-1.08861	-1.41619	-0.91812	-0.98993	2.34047	2.10755
$Gc = 4.0$	-0.033	-0.38186	-1.00681	-0.65769	-0.88175	0.75193	1.10227
$Gc = 8.0$	-0.033	0.65523	-0.66609	-0.91932	-0.84201	1.93193	0.64764
$Gt = 0.0$	-0.033	-0.76081	-1.19877	-0.73565	-0.91046	1.27271	1.43660
$Gt = 1.0$	-0.033	-1.20728	-1.81880	-1.22631	-1.26111	3.98580	3.65470
$Gt = 2.0$	-0.033	-1.58715	-2.30535	-1.61728	-1.52401	6.09261	5.22500
$M = 0.0$	0.100	-1.45265	-1.84405	-1.45510	-1.91622	2.23150	2.19474
$M = 2.0$	0.000	-0.97935	-1.40270	-0.96507	-1.22427	1.60144	1.72602
$M = 4.0$	-0.050	-0.67599	-1.14440	-0.65171	-0.76360	1.37285	1.50155
$m = 0$	-0.033	-0.77268	-1.23116	-0.59111	-0.83133	1.31566	1.54800
$m = 1$	-0.033	-0.81494	-1.24545	-1.29111	-1.33523	1.72188	1.66696
$m = 2$	-0.033	-0.82974	-1.25229	-1.65653	-1.66355	1.88328	1.73468
$\gamma = 0.0$	-0.033	-0.77184	-1.22643	-0.94441	-1.11262	2.36455	2.54620
$\gamma = 2.0$	-0.033	-0.79486	-1.24166	-0.55858	-0.72343	0.35773	0.44601

$\gamma = 4.0$	-0.033	-0.79202	-1.24225	-0.52225	-0.68428	0.16558	0.23216
$R = 6.0$	-0.033	-0.87959	-1.28102	-0.40833	-0.59798	-0.45035	-0.22712
$R = 20.0$	-0.033	-0.78500	-1.23442	-0.76357	-0.93142	1.42936	1.57338
$R = 40.0$	-0.033	-0.70280	-1.19382	-1.01873	-1.21790	2.80527	3.13507
$Ec = 0.0$	0.000	-0.80029	-1.25876	-0.78128	-0.97700	1.45147	1.60571
$Ec = 4.0$	-0.333	-0.66116	-1.03823	-0.61101	-0.55990	1.24031	1.31401
$Ec = 8.0$	-0.667	-0.55164	-0.86504	-0.45511	-0.24191	1.04231	1.08668

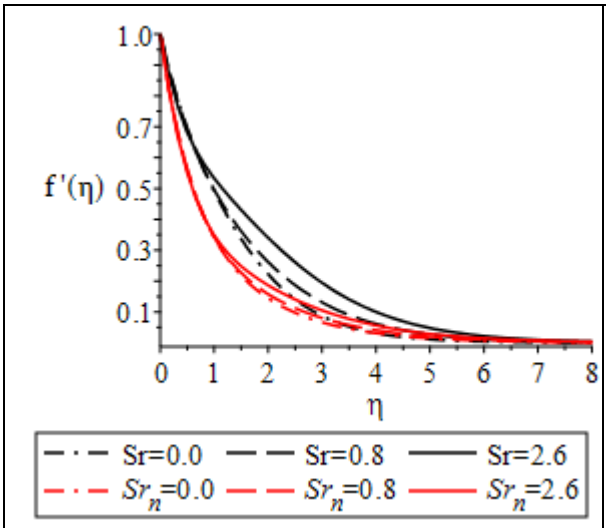

Fig. 2: Effects of Soret (Sr) on velocity profile

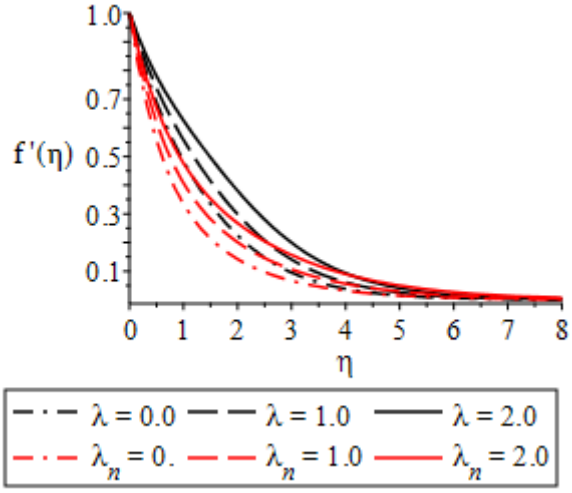

Fig.3: Effect of Stretching parameter on velocity profile.

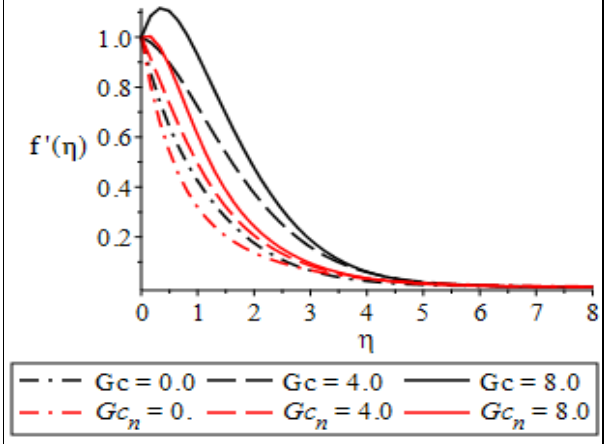

Fig.4: Effects of Buoyancy due to concentration parameter (Gc) on velocity

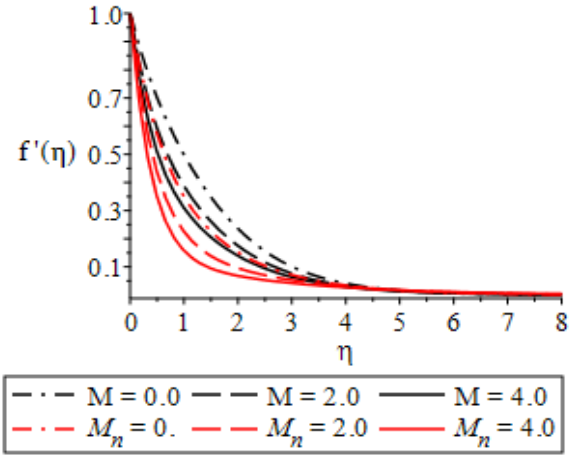

Fig.5: Effects of Magnetic Parameter (M) on velocity

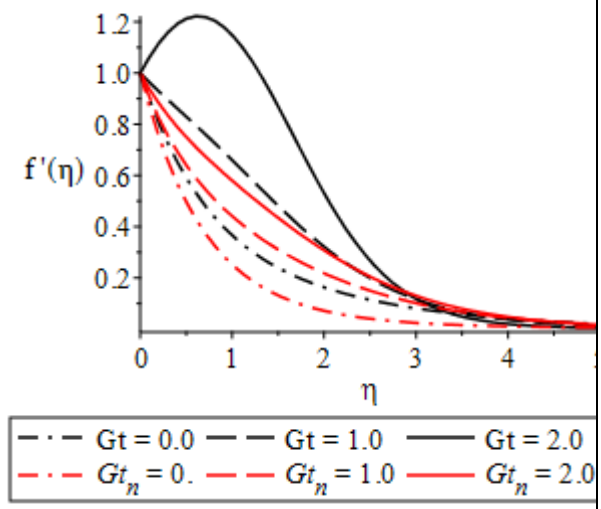

Fig.6: Effect of Buoyancy parameter (Gt) on velocity

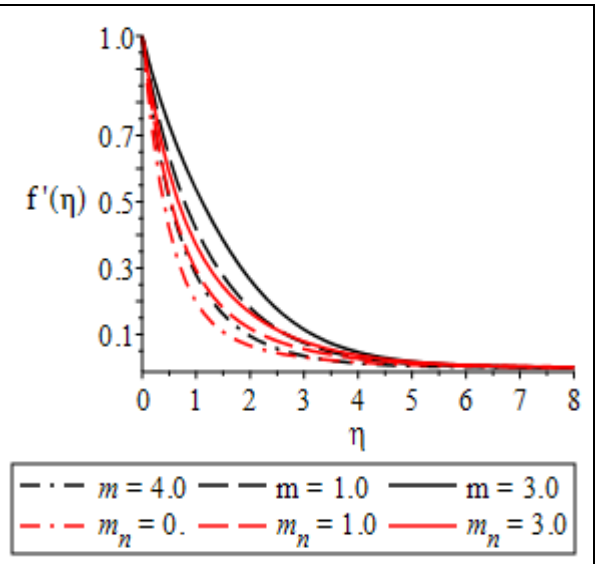

Fig.7: Effect of velocity index (m) on velocity

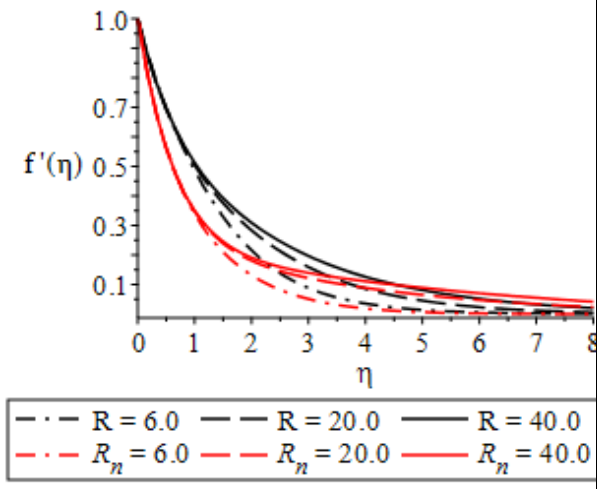

Fig.8: Effect of Radiating parameter (R) on velocity

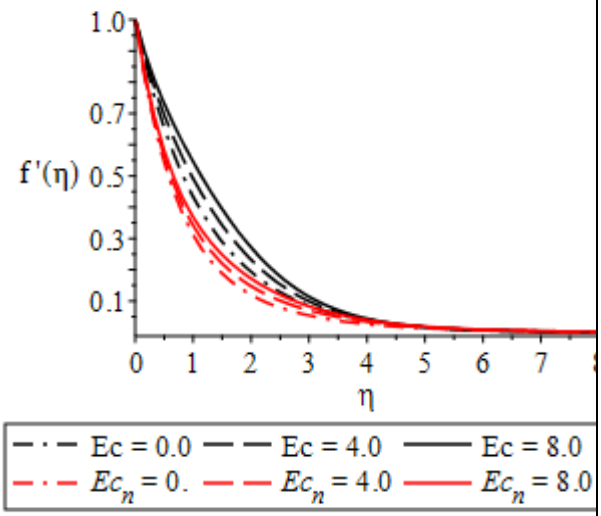

Fig.9: Effect of Eckert number (Ec) on velocity

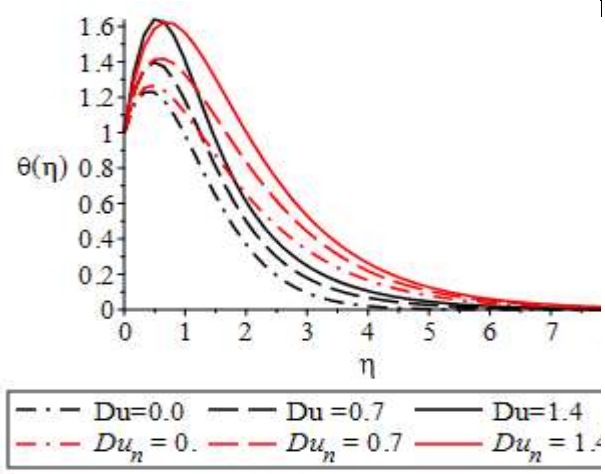

Fig.10: Effect of Dufour (Du) on Temperature distribution.

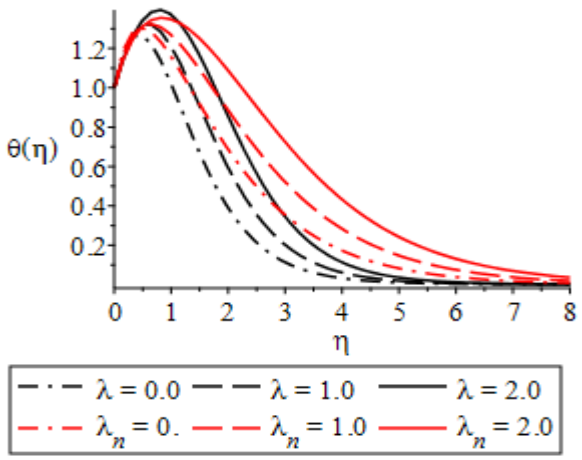

Fig.11: Effect of the stretching parameter on Temperature distribution.

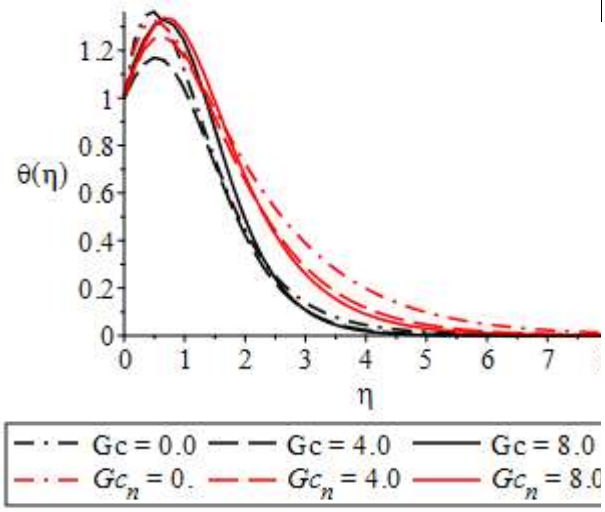

Fig.12: Effect of Buoyancy due to concentration (Gc) on Temperature distribution.

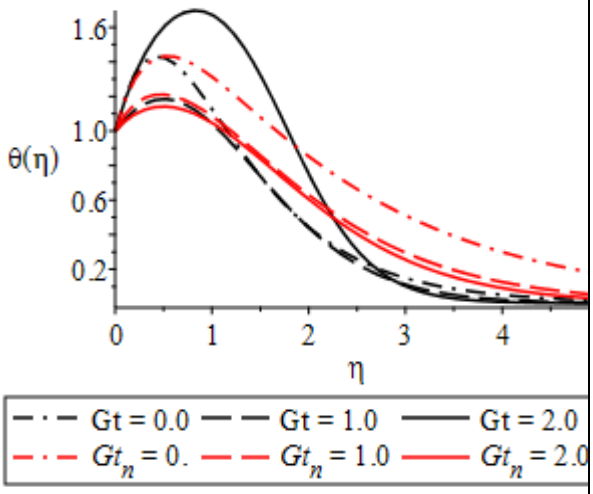

Fig.13: Effect of Buoyancy due to Temperature on Temperature distribution

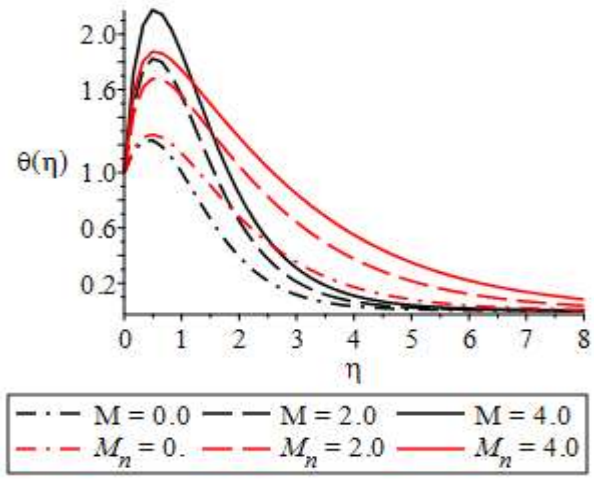

Fig.14: Effect of Magnetic parameter (M) on Temperature distribution

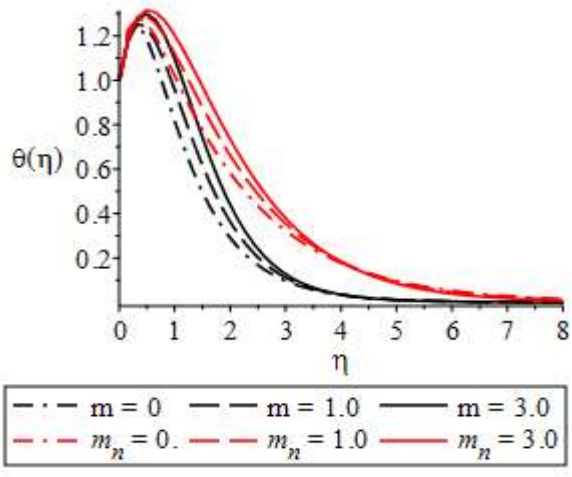

Fig. 15: Effect of velocity index (m) on Temperature distribution.

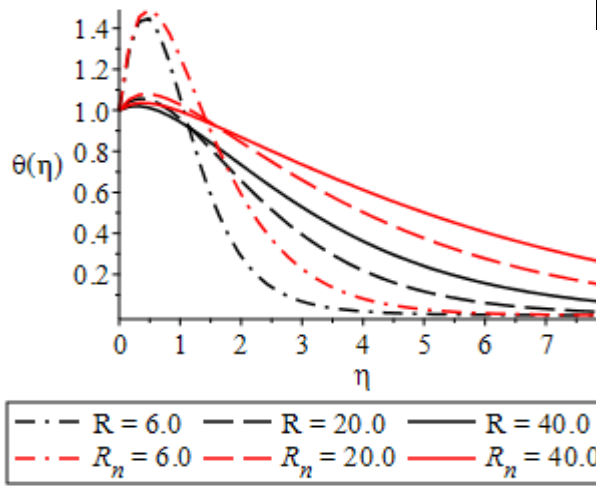

Fig.16: Effect of Radiating parameter (R) on Temperature distribution.

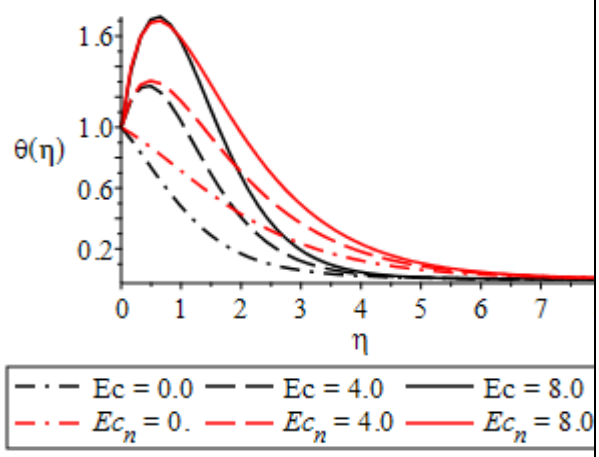

Fig.17: Effect of Eckert number (Ec) on Temperature distribution.

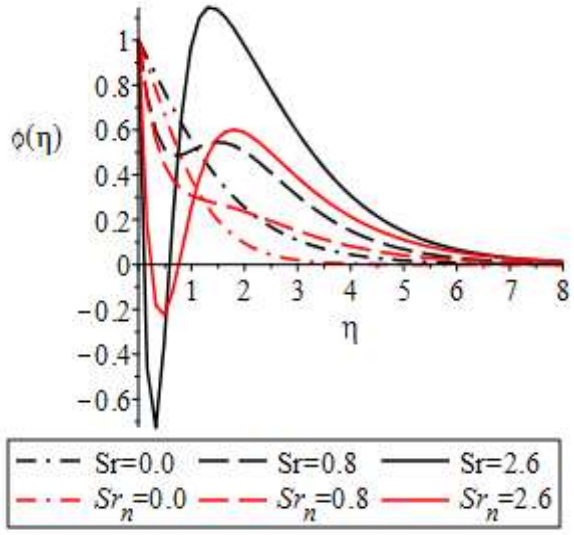

Fig.18: Effect of Soret (Sr) on Temperature distribution.

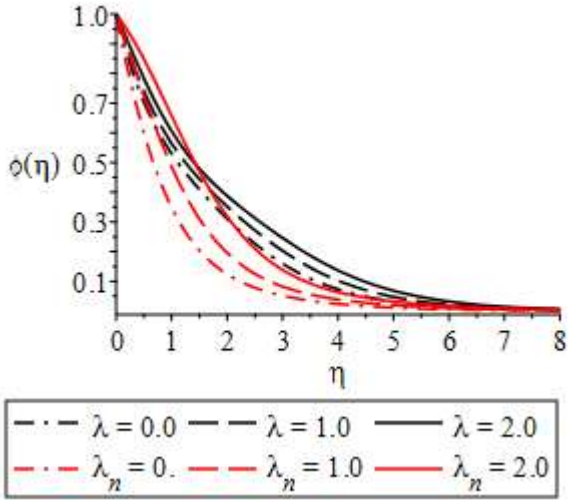

Fig.19: Effect of stretching sheet parameter on Temperature distribution.

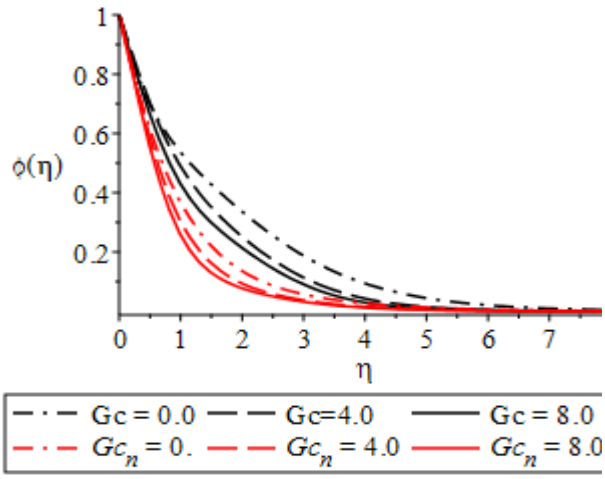

Fig.20: Effect of Buoyancy due to concentration on Concentration distribution.

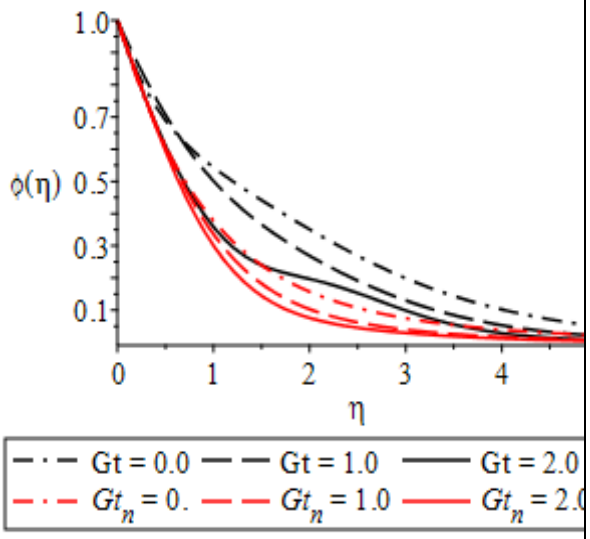

Fig.21: Effect of Buoyancy due to Temperture on Concentration distribution

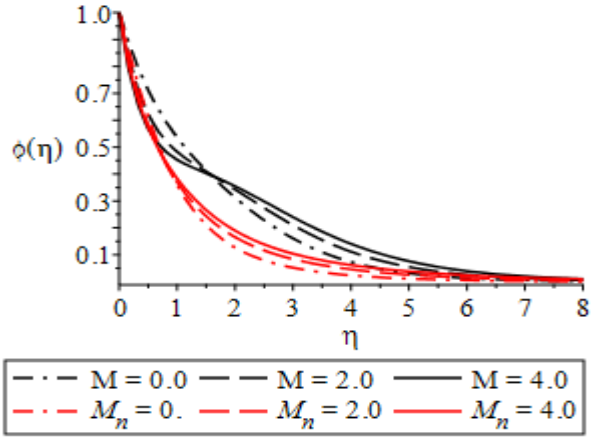

Fig.22: Effect of Magnetic parameter (M) on concentration distribution.

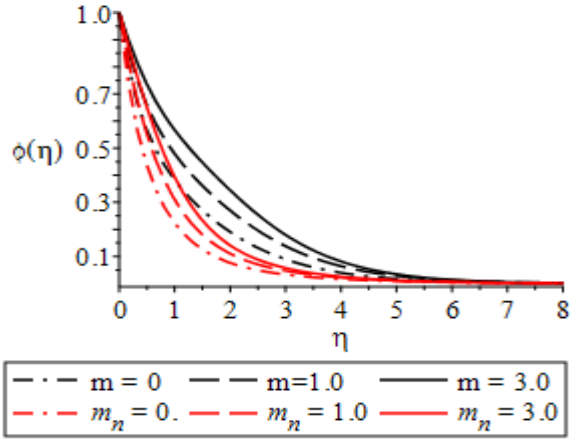

Fig.23: Effect of velocity index (m) on Concentration distribution.

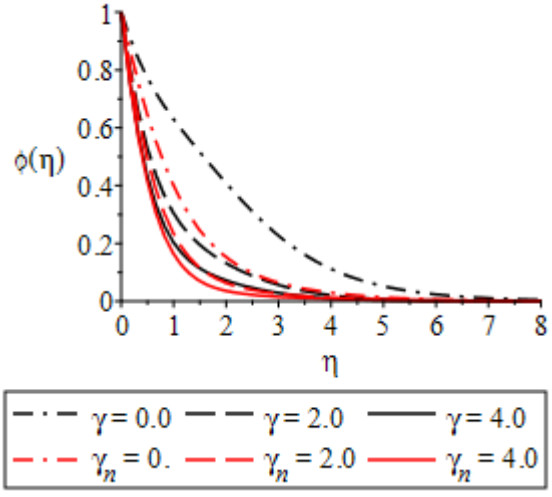

Fig.24: Effect of scaled chemical reaction parameter (γ) on Concentration disribution.

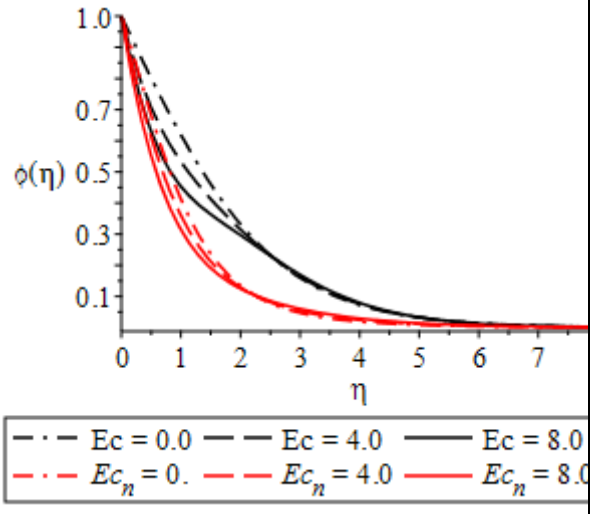

Fig.25: Effect of Eckert number (Ec) on Concentration distribution.

4. CONCLUSION

In this article, the impact of velocity index and significance of nanofluid flow of magnetohydrodynamics (MHD) over a stretching sheet with Dufour and Ohmic heating has been studied. The study was actually meant to examine the various effect of the controlling parameter on fluid flow and to show the significance of nanofluid thermophysical properties on heat and mass transfer. From the study the following conclusion has been drawn;

1. The increase in the velocity index parameter (m) causes an increase in the velocity, temperature and concentration of the fluid. This is due to the earlier fact pointed out in the introduction and the course of result discussion.
2. Nanofluid enhances the flow of fluids and improves the heat and mass transfer (i.e. enhances thermal conductivity) which is a significant measure in industrial processes.
3. The increase in the buoyancy due to concentration parameter (Gc) and temperature (Gt) respectively results in the increase of the velocity of the fluid.
4. The increase in the Soret number and the stretching sheet parameter leads to the increase in the velocity of the fluid and a decreasing function of mass transfer at the wall and an increasing function of mass transfer along the free stream. The increase in the scaled chemical reaction parameter (γ) causes a decreasing effect in the mass transfer. the increase in the Eckert number (Ec), causes a decrease in the mass transfer at some point from the wall to a point in the free stream and a little significant increase in the mass transfer at another point in the free stream.
5. The velocity of the fluid decreases as the Magnetic parameter (M) increases and there is a significant increase in temperature from the wall and all through to the free stream as there is an increase in the dufour number and the stretching sheet parameter.
6. There is a significant increase in the temperature at the wall and a decreasing effect along the free stream as there is an increase in the buoyancy due concentration parameter (Gc). Similarly, there is an increasing effect on temperature at the wall and a decreasing effect of temperature at the free stream since there is an increase in the buoyancy due temperature parameter (Gt).

References

Osimobi, J.C., Avwiri, G.O., & **Agbalagba E.O.** (2018). Radiometric and radiogenic heat evaluation of natural radioactivity in soil around solid minerals mining environment in South-eastern Nigeria. *Springer, Environmental Process 5(4), 860-877.*

Abu-Nada, E. (2009) "Effects of variable viscosity and thermal conductivity of Al_2O_3water nanofluid" *Int. J. Heat Fluid Flow* (2009), doi: 10.1016/j.ijheatfluidflow.2009.02.003 .

Alfven, H. (1942). Existence of Electromagnetic-Hydrodynamic Waves. *Nature Publishing Group*, 150(3805), 405-406.

Amireh, N., Hamdolah, M. and Morteza, B., (2019), "Effect of radiation and Magnetohydrodynamics (MHD) on heat Transfer of nanofluid flow over a plate" SN Applied sciences (2019)

|:1581|https://doi.org/10.1007|s42452-019-1634-6

Angue M, Roy HG, Nguyen CT and Doucet D (2009) "New temperature and conductivity data for water-based nanofluids". *Int. J. Therm. Sci. 48* (2), 363–371,

Animasaun I. L. and Sandeep, N., (2016)."Buoyancy induced model for the flow of 36 nm alumina-water nanofluid along upper horizontal surface of a paraboloid of revolution with variable thermal conductivity and viscosity" *Power Technology* **301**, 858 - 867. doi: /10.1016/j.powtec.2016.07.023

Bhavin M, Dattatraya S., Hitesh P and Zafar S. (2022) "Synthesis, Stability, Thermophysical Property and Heat Transfer Applications of Nanofluid – A Review", *Journal of molecular liquids* 364, https://doi.org/10.1016/j.molliq.2022./20034

Bharat B. and Divya B. (2021) "Nonofluids for Heat and Mass Transfer" *Sciencedirect* https://doi.org/10.1016/B978-12-821955-3.0001-x

Durga, P. P. and Varma, S. V. K. (2018), "Heat and Mass Transfer Analysis for the MHD flow of nanofluid with radiation absorption", *Ain shams Engineering journal*, .9, 801 – 813. https://doi.org/10.1016/j.asej.2016.04.016

Eshetu, H. and Shankar, B. (2015). A Steady MHD Boundary Layer Flow of Water-base Nanofluids overa Moving Permeable Flat Plate. *International Journal of Mathematical Research*, 4(1): 27 – 41

Hunegnaw, D. and Nailoti, K. (2014), "MHD effect on heat transfer over stretching sheet embendded in porous medium with variable viscosity, viscous dissipation and heat source/sink", *Ain shams Engineering journal*,.9, 01–13. https://doi.org/10.1016/j.asej.2014.03.008

Javad A. and Samarbakhsh (2012) "Viscous Flow Over a Nonlinear Stretching Sheet with Effects of Viscous Dissipation", *Journal of applied Mathematics*, https://doi.org/10.1155/2012/587834

Hassan Y. (2017) "An Overview of Computational Fluid Dynamics and Nuclear Applications, thermal-hydraulic of water-cooled Nuclear Reactor" Page 279-829, doi.org/10.1016/B978-0-08-10062-7.00012-9.

Husseini, M. A. (2013). Radiation Effect on Mixed Convection along a Vertical Plate With Uniform Surface Temperature. *Journal of Heat and Mass Transfer*, 31, 243-248.

John H. M, Ioan P., Yian Y. L. and Teodor G. (2022) "Convective flow with Internal Heat Generation in Porous Media" *ScienceDirect* page 205 – 223, https://doi.org/10.1016/B97-0-12-821188-5.0004-7.

Johnson E. D. and Cowen (2017), "Remote Determination of the Velocity Index and Mean Streamwise Velocity Profiles". *Water Resource Research*,.53(9), 7521-7535, https://doi.10.1002/2017WR020504

Kalaivanan K., Vishnu G. and Qasem M. A. (2021) "Buoyancy Driven Flow of a Second-Grade Nanofluid flow taking into Account the Arrhenius Activation

Energy and Elastic Deformation" doi.10.32604/fdmp.2021.012789

Khan, I. and Alqahtani, A. M. (2019), "MHD nanofluid in a permeable channel with porosity", symmetry 2019, 11,378; doi:103390/sym11030378.

Koriko O. K., Omowaye A. J., Animasaun I. L. and Sandeep N. (2017), "Analysis of Boundary Layer formed on an Upper Horizontal Surface of a Paraboloid of Revolution within Nanofluid Flowing the Presence of Thermophoresis and Brownian Motion of 29nm Cuo.", *Internatioal Journal of Mechanical Science*, 124-125, 22-36, http://dx.doi.org/10.1016/j.ijmecsci.2017.02.020

Lakshmi, G. D., Niranja, H. and Sivasankara, S. (2021), "Effects of chemical reaction, radiation and activation energy on MHD buoyancy induced nanofluid flow past a vertical surface", *Transsaction B: Mechanical engineering, scientific Iranica B* (2022) 29(1), 90-100, DOI: 10.24200sci.56835.4934

Liu, M., Lin, M. C. and Wang, C. (2011) "Enhancements of thermal conductivities with Cu, CuO, and carbon nanotube nanofluids and application of MWNT/water nanofluid on a water chiller system." *Nanoscale Research Letter* 6, 297. doi:10.1186/1556-276X-6-297.

Manjunatha, S and Gieesha, B. J. (2015) "Effects of Variable Viscosity and Thermal Conductivity on MHD flow and heat Transfer of a Dusty Fluid" *Ain shams Engineering Journal* http://dx.doi.org/10.1016/j.2015.01.006

Makinde, O. D. and Animasaun, I. L. (2016),"Bioconvection in MHD nanofluid flow with nonlinear thermal radiation and quartic autocatalysis chemical reaction past an upper surface of a paraboloid of revolution," *International Journal of Thermal Sciences* **109**, 159 - 171.

Mintsa, H. A., Nguyen CT and Roy G (2007),"New Temperature Dependent Thermal Conductivity Data of Water Based Nanofluids," *Proceedings of the 5th IASME/WSEAS Int. Conference on Heat Transfer, Thermal Engineering and Environment, Athens, Greece* **290**, 25-27.

Munish G., Vinay S. Rajesh K. and Said Z. (2017) "A Review of Thermophysical Propeties of Nanofluid and Heat Transfer Application", Sciencedirect, 74, 638 – 670, https://doi.org/10.1016/j.ser.2017.02.73

Musa, A. M., Verdiana, G. M., Eunice, W. M. and Makungu, N. J. (2019), "Unsteady MHD flow nanofluid with variable properties over a stretching sheet in the presence thermal radiation and chemical reaction", international journal of mathematics and mathematical science.

Nguyen, C. T., (2012), "Fundamentals of Mass Transport in microscale,"., second edition, http://doi.org/1016/B978 - 1 - 4377-3520-8.00002 – 4.

Nguyen CT, Desgranges F, Roy G, Galanis N, Mare T, Boucher S and Angue Minsta H, (2007), "Temperature and particle-size dependent viscosity data for water based nanofluids – hystresis phenomenon". *Int. J. Heat Fluid Flow* 28, 1492–1506.

Okedoye A. M., Ogboru O. K. and Damisa J. S. (2022). "Two Dimensional Dissipative Non-Slip Magnetohydrodynamic(MHD) Flow of Arrhenius Chemical Reaction with Variable Properties." (pp:357-371www.ijaem.net ISSN: 2395-5252)

Okedoye A. M., Damisa J. S., Malemi B. and Ogboru O. K. (2022), "Buoyancy Effect on MHD Nanofluid flow over a Porous Medium in the Presence of Dufour and Ohmic Heating", *IOSR Journal of Mathematics,* DOI: 10.9790/5728-1802022639.

Salengke, S. (2000). Electrothermal Effects of Ohmic Heating on Biomaterials Temperature Monitoring, Heating of Solid-Liquid Mixtures and Pretreatment Effects on Drying Rate and Oil Uptake. *Unpublished Ph.D. Dissertation. The Ohio State University, United States of America.*

Sastry, S. k and Palaniappan, S, (1992). Ohmic Heating of Liquid-particle Mixtures, *Journal of Food Technology*, **46**, 64–70.

Shankar, B. and Eshetu, H. (2014). Heat and Mass Transfer through a Porous Media of MHD Flow of Nanofluid with Thermal Radiation, Viscous Dissipation and Chemical Reaction Effect. *American Chemical Science Journal*, 4(6), 828-846.

Subhas, M. A., Klkarni, A. K. and Ravikumara, R., (2011), "MHD flow and heat transfer with effects of buoyancy, viscosity and Joules dissipation over a nonlinear vertical stretching porous sheet with partial slip".3(3), Doi:10.4236/eng.2011.33033

Raptis, A. (1998). Radiation and Free Convection Flow through a Porous Medium. *International Communication in Heat and Mass Transfer*. 25, 289-295.

Vikas Poply (2020) "Heat Transfer in MHD Nanofluid over a Stretching Sheet", doi:10.5772/intechopen.95387.

Yahaya, S. D. and Simon, K. D., (2015), "Effect of Buoyancy and Thermal Radiation on MHD flow over a Stretching Porous Sheet using Homotopy Analysis Method".

Yinnin X and Qiang L. (2000) "Heat transfer Enhancement of Nanofluid" *International journal of Heat and Fluid flow* 21(1), 58 – 64, https://doi.org/10.1016/50142-727x(99)00067-3.

Appendix
Nomenclature

Parameter	Definition		Parameter	Definition
k_1	Porous medium parameter		$\boldsymbol{Ec}$	Eckert number
$\boldsymbol{Grt}$	Buoyancy coefficient factor		$\boldsymbol{l}$	Characteristics length
$\boldsymbol{S_G}$	Ratio of Nanofluid particle and base fluid		$\boldsymbol{T_\infty}$	Ambient temperature
$\boldsymbol{R_d}$	Thermal radiation parameter		$\boldsymbol{C_\infty}$	Ambient concentration
$\boldsymbol{A}$	Area of emitting body of temperature		η	similarity variable
$\boldsymbol{D_1}$			Pr	Prandtl number
$\boldsymbol{Sr}$	Soret number		M	magnetic parameter

$\boldsymbol{B}$	Area of emitting body of concentration		Sr	Soret number
τ_w	shear stress at the surface		Sc	Schmidt number
q_w	heat flux at the surface		R_d	Radiation parameter
J_w	mass flux at the surface		Ec	Eckert number
$\boldsymbol{k_1}$	Porous medium parameter		Grt	coefficient respectively
$\boldsymbol{Grc}$	Buoyancy coefficient ratio		$\boldsymbol{Du}$	Dufour number
$\boldsymbol{R}$	Thermal radiation parameter		$\boldsymbol{T_w}$	wall temperature
$\boldsymbol{k_{nf}}$	Thermal conductivity of Nanofluid		$\boldsymbol{C_w}$	Wall concentration
γ	Scaled chemical reaction parameter		$\boldsymbol{Sc}$	Schmidt number
			$\boldsymbol{D_m}$	Mass diffusivity